

REPORT DOCUMENTATION PAGE

AFRL-SR-AR-TR-09-0067

Public Reporting burden for this collection of information is estimated to average 1 hour per response, including the time for reviewing instructions, searching existing data bases, gathering and maintaining the data needed, and completing and reviewing the collection of information. Send comment regarding this burden estimates or any other aspect of this collection of information, including suggestions for reducing this burden, to Washington Headquarters Services, Directorate for information Operations and Reports, 1215 Jefferson Davis Highway, Suite 1204, Arlington, VA 22202-4302, and to the Office of Management and Budget, Paperwork Reduction Project (0704-0188,) Washington, DC 20503.

1. AGENCY USE ONLY (Leave Blank)		2. REPORT DATE 5/15/08		3. REPORT TYPE AND DATES COVERED Final Technical Report 09/03-04/08	
4. TITLE AND SUBTITLE Type-II Superlattice for High Performance LWIR Detectors				5. FUNDING NUMBERS F49620-03-1-0436	
6. AUTHOR(S) M. Razeghi					
7. PERFORMING ORGANIZATION NAME(S) AND ADDRESS(ES) Northwestern University Center for Quantum Devices 2220 Campus Drive, Room 4051 Evanston, IL 60208				8. PERFORMING ORGANIZATION REPORT NUMBER 0650-350-S444	
9. SPONSORING / MONITORING AGENCY NAME(S) AND ADDRESS(ES) U.S. Air Force Office of Scientific Research 875 N. Randolph Street Arlington, VA 22203-1954				10. SPONSORING / MONITORING AGENCY REPORT NUMBER AFRL-SR-AR-TR-08-0549	
11. SUPPLEMENTARY NOTES The views, opinions and/or findings contained in this report are those of the author(s) and should not be construed as an official Department of the Air Force position, policy or decision, unless so designated by other documentation.					
12 a. DISTRIBUTION / AVAILABILITY STATEMENT Approved for public release; distribution unlimited.				12 b. DISTRIBUTION CODE	
13. ABSTRACT (Maximum 200 words) We have studied and reported on the temperature dependant photoluminescence of Type-II InAs/GaSb superlattices. The PL spectrum gives precise information on the energy levels available to the electrons. The intensity of the PL signal depends on the rate of the radiative and non – radiative events that in turn depends on the density of the non – radiative states. We look at the bangap dependence excitation intensity dependence of the Photoluminescence of a variety of Type-II superlattices. We then study the properties of MWIR Type-II superlattices in more detail, studying the temperature dependence extensively and develop models for the superlattice behavior.					
14. SUBJECT TERMS				15. NUMBER OF PAGES 26	
				16. PRICE CODE	
17. SECURITY CLASSIFICATION OR REPORT UNCLASSIFIED		18. SECURITY CLASSIFICATION ON THIS PAGE UNCLASSIFIED		19. SECURITY CLASSIFICATION OF ABSTRACT UNCLASSIFIED	
				20. LIMITATION OF ABSTRACT UL	

Final Technical Report

Type-II Superlattice for High Performance LWIR Detectors

Contract No: F49620-03-1-0436

(9/03 – 4/08)

Program Managers:

Dr. Vaidya Nathan – Air Force Research Laboratory

Dr. Donald Silversmith – Air Force Office of Scientific Research

Principal Investigator: Professor Manijeh Razeghi

Graduate Students: Binh-Minh Nguyen, Darin Hoffman, Pierre-Yves Delaunay, Ed Huang,

Center for Quantum Devices

Electrical and Computer Department

Northwestern University

2220 Campus Dr. Cook Hall Rm. 4051, Evanston, IL 60208

Tel: (847) 491-7251, Fax: (847) 467-1817

Email: razeghi@eecs.northwestern.edu

20090324164

I. Introduction

Photoluminescence (PL) is the spontaneous emission of light from a material under optical excitation. The excitation energy and intensity of the probe excitation source are chosen to probe different regions and characterize a variety of the material properties. PL studies can be used to characterize material parameters without harming or degrading a sample. PL spectroscopy provides electrical, as opposed to mechanical, characterization; features in the emission spectrum can be used to identify surface, interface, impurity levels, and gauge alloy disorder or interface roughness. The intensity of the PL signal provides information on the quality of surfaces, interfaces, and epitaxial layers. Under pulsed excitation, the transient PL intensity can be used to model the lifetime of non-equilibrium interface and bulk states. Variation of the PL intensity as a function of location can be used to map the uniformity of the epitaxial layer growth of a sample. In addition, thermally activated processes cause changes in PL intensity with temperature.

PL analysis is a non-destructive technique requiring very little sample manipulation or environmental control. Since the sample is excited optically, electrical contacts and junctions are not required, and the materials resistance does not pose a measurement limitation. In addition, PL spectroscopy can be very fast making it useful for characterizing and comparing material in a rapid and repeatable way. The fundamental limitation of PL analysis is its reliance on attaining and measuring radiative events. Materials with poor radiative efficiency, such as indirect bandgap semiconductors, materials with very narrow band gaps, or materials with rough interfaces are difficult to study via ordinary PL. Similarly, identification of impurity and defect states depends on the optical activity; so if they are weak in comparison to the primary excitonic emissions states they may not be visible or differentiable. Finally, if there are states that do not couple strongly with light, secondary analysis or multiple probe techniques are required to probe these levels.

II. Theory for PL

The primary purpose for designing multilayer structures is to change the potential energy of the electrons and holes; making the band structure different than its constituents. Since

interactions at the interfaces and surfaces tend to dominate, the behavior of these devices is limited by the heterojunctions. Smooth and atomically abrupt interfaces are required for good optical and electrical performance. Even more importantly, defects and impurities at the interfaces provide new states for electrons and holes, altering their motion, lifetime, and transition energies.

When light of sufficient energy is incident on a material, photons are absorbed and electronic excitations occur. Eventually, these excitations relax and the electrons return to their ground states. If radiative relaxation occurs, then the emitted light is photoluminescence. This light can be collected and analyzed to yield information about the photo-excited material. The PL spectrum provides the transition energies that can be used to determine the electronic energy levels. The PL intensity gives a measure of the relative rates of radiative and non-radiative recombination. Variation of PL intensity with external parameters like temperature and electromagnetic field can be used to characterize further underlying electronic states and bands.

PL depends on the nature of the optical excitation. The excitation energy selects the initial photo excited state and governs the penetration depth of the incident light. The PL signal depends directly on the amount of the photo-excited carriers and can usually be increased by increasing the intensity of the incident beam. When the type or quality of material varies spatially, the PL signal will change with excitation position. In addition, by performing pulse optical excitation transient phenomena can be identified, this is due to the fact that short laser pulses produce an instantaneous excited population, and given a high speed detector, the PL signal can be observed to change based upon the inherent recombination rates.

PL is simple, versatile, and non-destructive. The instrumentation that is required for PL work is unremarkable: an optical source, a spectrometer, and a detector. In Figure 1, a typical PL set up is shown, since the measurements do not rely on electrical excitation or detection, sample preparation is minimal. Measuring continuous wave PL intensity and spectrum is quick and straightforward, while measuring transient PL is more complicated. This is especially true when the recombination processes are fast (on the order of nanoseconds or less); in this case high speed time-resolved detection is required; making the measurement setup expensive and complex.

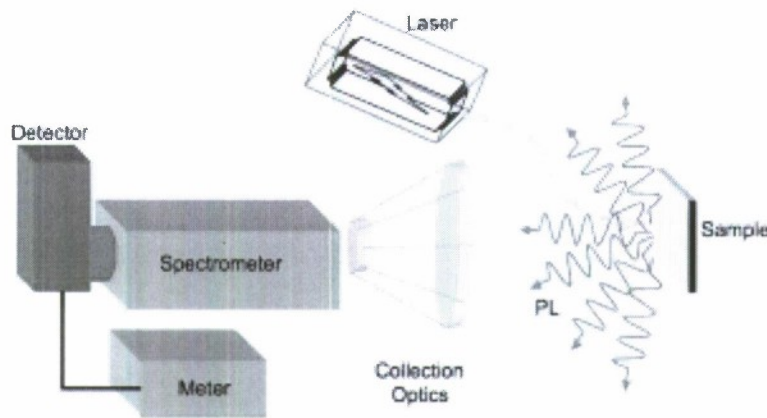


Figure 1: Basic experimental setup required for PL measurements.

The advantages of PL analysis are derived from the simplicity of optical measurements and the power to probe fundamental electronic properties. PL can be used to study virtually any material in any environment; it is generally not sensitive to the pressure or environmental condition of the sample under investigation. Although PL does depend strongly on temperature, liquid helium temperatures being required for the highest spectral resolution, while room temperature measurements are sufficient for many purposes. In addition, PL has little effect on the sample under investigation; photo - induced changes, such as heat are possible, but maintaining low excitation energies can minimize these effects. This allows for an epitaxial grown structure to have PL performed and then processed (defining mesas photodiodes) and not deleterious effect its operability. Compared to other optical measurement, reflection and absorption, PL is less stringent on sample alignment, surface flatness, material thickness, and substrate.

The main drawback of PL analysis follows suit from the reliance on the optical technique; i.e., the sample under investigation must emit light. Indirect bandgap semiconductors have inherently low PL efficiency since the conduction band minimum is separated from the valence band maximum in momentum space. In samples that non - radiative recombination dominates, such as indirect band gap materials, the relaxation of the excited carriers from luminescence is often too low to discern from background noise. Nevertheless, once the PL signal is detected, it can be used to characterize both the radiative and non-radiative transitions. Another inadequacy of PL is the difficulty in estimating the density of interface and impurity states. When these states have radiative levels, they are easily identified in the PL spectrum, and

the intensity of the peak can provide a relative measure of their presence. However, measuring the absolute density of these states or any other is a far more complex task and typically requires an exhaustive analysis of the excitation source, the measurement set up, the penetration depth, and the excited carrier mobility as function of the PL signal strength.

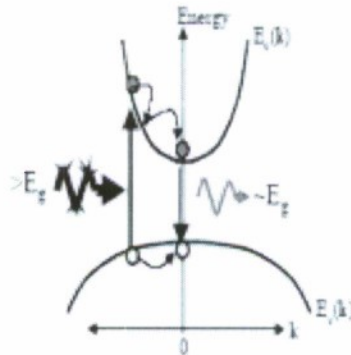


Figure 2: Schematic diagram of carrier relaxation in a direct bandgap semiconductor.

As shown in Figure 1, the measurement setup for PL can be a rather simple design: a sample is excited with an optical source, typically a laser with an emission wavelength greater than the bandgap ($h\nu > E_g$) generates electron – hole pairs that recombine by one of several mechanisms. Photons are emitted from radiative recombination (Figure 2), for non – radiative processes photons are not emitted. For high quality PL, the goal is to have the majority of the recombination processes to be radiative. The emitted photon energy depends on the recombination process as illustrated in Figure 3, where the commonly observable PL transitions are shown [1].

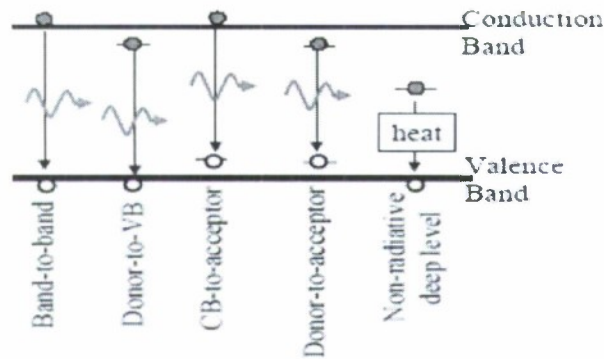


Figure 3: Radiative transitions observable from photoluminescence spectroscopy.

III. Photoluminescence Spectrum

Optical transitions provide a direct technique to probe the energy levels within a system; due to the fact that the photons of a particular energy that are absorbed or emitted by a sample provide evidence of the electronic states differing by the energy within the material. Absorption is a good probe of overall band structure of a system because bands have a relatively high density of states; where in comparison, PL emission tends to favor sparse low – lying states because photo - excited carriers rapidly thermalize through bands and closely spaced states. This makes PL particularly effective in analyzing interfaces where discrete defect and impurity states exist. If the state is radiative, it will generate unique peaks in the PL spectrum. Thus, the PL measurement is a very sensitive tool to probe such states.

A. PL Peak Positions

In the bulk crystalline material, the translational symmetry leads to the formation of electronic energy bands. Defects and impurities break the periodicity of the lattice, thereby disturbing the band structure locally. The perturbation is often characterized by discrete energy levels within the bandgap. In a similar fashion, a superlattice forms mini – bands due to the layering thickness of the individual materials and from these minibands the bandgap is formed. As a pseudo-bulk material, defects and impurities will perturb the band structure on the local level. In general though grown in defects are quite small, but a more serious form of defects that is experienced in

structured materials comes from the interfaces of the layers. Local stresses at the interfaces causes inter – diffusion of atoms or interface roughness, caused when the individual layers do not have identical lattice constant; thereby, perturbing the global band structure. With high quality materials, this interface roughness is minimal and not readily distinguishable except at low temperature regimes.

When the temperature is sufficiently low, carriers can be trapped at these states. If these carriers recombine radiatively, the energy of the emitted light can be studied to determine the energy of the defect level. Shallow impurity levels, those near the band edge of either the conduction or valence band, are more likely to radiatively recombine as long as the sample temperature is low to prevent these carriers from being thermally activated out of the traps. Deep level traps tend to act as intermediate states for the recombination of the electrons and holes and either emits photons at very low levels or none at all. In Figure 3, there are several of the possible transitions that can occur during recombination.

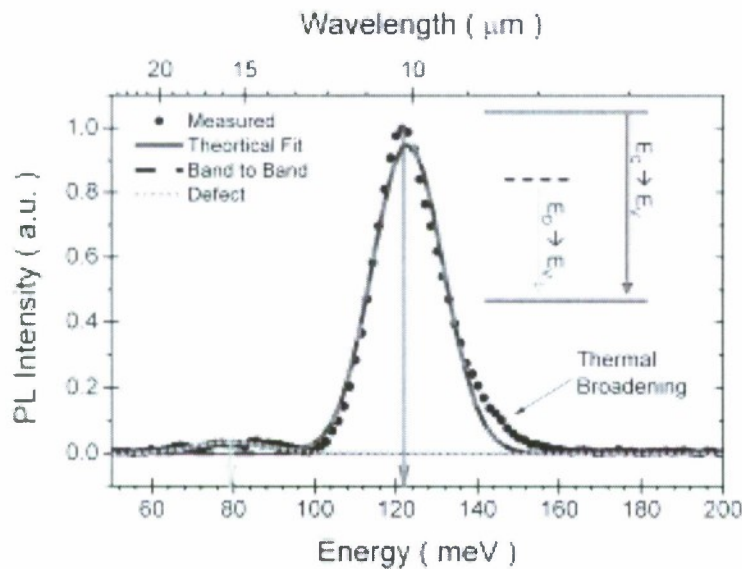


Figure 4: Photoluminescence of LWIR sample that was grown without doping.

Figure 4 shows the normalized PL spectrum of a LWIR T2SL sample with layer design of 9 MLs InAs to 3 MLs GaSb. At approximately 10 μm , there is the primary peak, which is

equivalent to the theoretically expected value from the layer design. Upon careful inspection in the lower energy side, there appears to be a secondary smaller peak at 79.5 meV (approximately $2/3 E_g$). This peak is attributed to the radiative recombination of donor defect to the valance band.

$$I = I_0 + \frac{A}{w\sqrt{\pi/2}} \exp\left(-2\frac{(x-x_c)^2}{w^2}\right) \quad \text{Equation 1}$$

$$FWHM = \frac{w}{\sqrt{\ln 4}}$$

The theoretical fits (the green line for donor recombination and the blue line for band to band recombination) in Figure 4 are modeled using a normal distribution, a Gaussian model, as described in Equation 1 where A is the amplitude, I_0 is the intensity offset, x_c is the center of the peak, and w is the full width of the peak. To convert from the full width to the full width at half the maximum (FWHM) the second equation is utilized.

B. PL Peak Broadening

When the light is incident on a semiconductor, photo – excitation of electrons from the valence to the conduction band will occur for any photon energy exceeding the bandgap. In this process, the difference between the excitation energy and the bandgap goes into the kinetic energy of the photo - excited carriers; thereby, the initial energy distribution of the electrons and holes depends upon the energy conservation not the temperature and the original carrier populations. To illustrate this point, imagine that the excitation energy is much greater than the bandgap, the electrons and holes created in their respective bands will have kinetic energies in excess to the characteristic thermal energy of the lattice that is related to k_bT and the formed electron – hole pairs will thermalize due to excess energy in the lattice. In the absence of Fermi filling events, they will settle into the standard Boltzmann distribution above their respective band edges; the conduction band for electrons and valence band for holes.

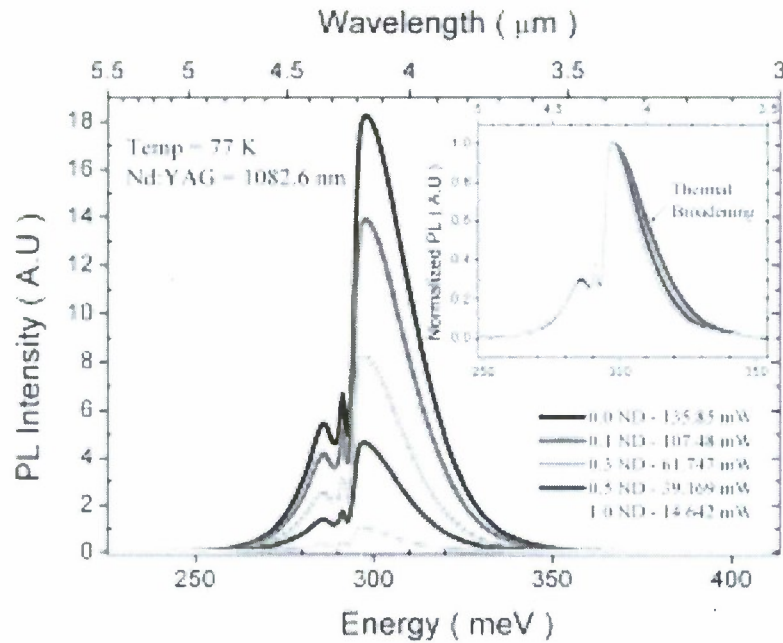


Figure 5: PL spectrum versus laser excitation intensity at 77 K. The intensity was adjusted by inserting a neutral density filter in the laser path. The inset shows the PL spectrum normalized to the peak, in the higher energy side thermal broadening is visible.

Since thermal broadening of the PL spectrum always occurs in timescales higher than the recombination time, thermal distribution is usually always observed in ordinary PL. Figure 5 shows the PL spectrum of a MWIR T2SL measured at 77 K. By increasing the laser power the PL intensity increases, but also in the higher energy side of PL spectrum (shorter wavelength) there is slight amount of thermal broadening. The inset of Figure 5 shows the PL spectrum normalized to the peak maximum, by increasing the laser excitation intensity by an order of magnitude the FWHM increases by approximately 0.52 meV. By understanding that the PL broadens with increased laser power, this can help to determine the thermal occupation of the available states by comparing the broadening with temperature dependent measurements. In this way, a qualitative measure of the lattice temperature as a function of excitation intensity is deduced.

IV. Photoluminescence Intensity

Of greatest significance of characterizing PL is the analysis of the PL intensity; this is based upon the fact that several key mechanisms effect the PL response. It is a general rule of thumb that the larger the PL signal, the better the material quality. For example, surface recombination acts as a non – radiative recombination channel or can bend the conduction and valence bands forming a depletion region where the PL emission is effectively quenched. In both these cases, the PL intensity is effectively reduced and this region acts as “*dead layer*”. Via PL alone determining what effect is changing the PL is complicated and requires a supplemental measurement.

A. Bandgap Dependence

In Figure 6 is a set of the integrated intensity of the measured PL for several samples spanning in wavelength from 4 to 25 μm . The PL intensity decreases as the bandgap shrinks. This is an expected trend for two reasons: first as the bandgap decreases the likelihood of the carrier to thermalize and not recombine radiatively increases and assuming all other values remain constant, the radiative lifetime decreases exponentially with decreasing bandgap. This is a similar trend to what occurs with the differential resistance of IR detectors with decreasing the bandgap in the energy scale.

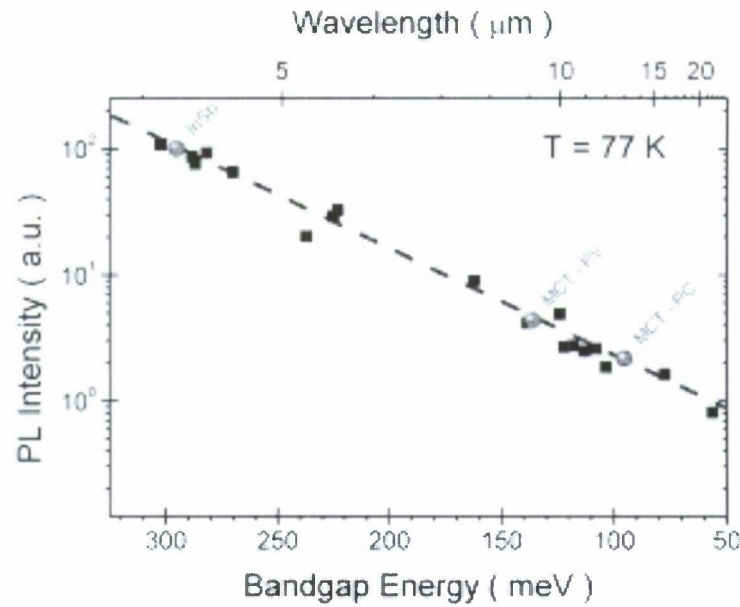


Figure 6: Plot of PL Intensity vs. cutoff wavelength measured at 77 K. The Red circles are the reference samples used for comparing the results for the each detector.

The red circles in Figure 6 are the reference samples that are measured at the same time as new samples using the specified detectors. This allows samples to be referenced over time and insure the material being compared from growth cycle to cycle is accurate by removing the variability of the measurement setup.

B. PL Intensity vs. Excitation Intensity

The intensity of the incident light (laser power) controls a critical property of the PL measurement: the density of the photo - excited electrons and holes. When the carrier density is low, the measurement is dominated by discrete defect and impurities at the interfaces the surface and within the bulk of the excited material. Recombination at these sites is refereed to as Shockley – Read – Hall recombination (SRH). The SRH rates are directly proportional to the dominant carrier density (n); where the dominant density is the greater of dopant type in the equilibrium carrier concentration and the photo –excited carrier concentration. In the intermediate excitation, the discrete states are filled and the bulk radiative recombination plays a more significant role. If the excitonic effects are ignored, the transitions are a two – body action

between the free electrons and holes, while the radiative recombination varies as the square of the concentration (n^2). In the third regime, high carrier densities, the three – body Auger process can become apparent; thereby, the rate would have dependence of the cube of the concentration (n^3).

Figure 7 shows the measured PL intensity dependent on the excitation intensity for a MWIR sample at both 10 and 77 Kelvin. To ensure that the spot size of the laser did not change with increasing the laser power, the laser power was kept at a stable value and series of neutral density filters were used to reduce the laser intensity without changing the laser’s Gaussian beam shape or width. At 10 K the PL has dependence of n^2 , as described above, which is an indication that the PL is from a band-to-band (purely excitonic) transition. As the temperature of the sample increases the dependence begins to decrease, this indicates that at higher temperatures the material is becoming more susceptible to the impurities. In addition at 10 K the PL starts at almost zero laser power when extrapolated zero intensity; this is opposite of the sample at 77 K.

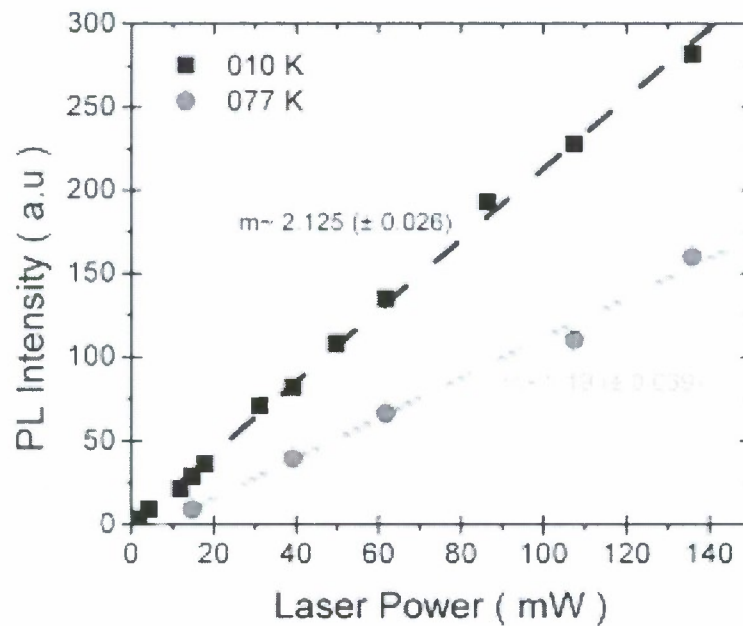


Figure 7: Plot of the measured integrated intensity vs. laser power at 10 K and 77 K.

The PL signal will not begin without a small offset in the laser power (x –axis); this is from a dead layer that is forming in the sample. In the surface of the sample, the PL there is a non –

radiative mechanism preventing the PL that needs to be satisfied prior to the PL signal from being developed. This may be from surface affect, such as surface leakage or band bending.

V. PL Temperature Dependence

The variation of the fundamental bandgap energy is an extremely important characteristic of any semiconductor material. By monitoring the change in the bandgap as a function of temperature, it brings forth important information not only in the material quality and fundamental limitation of the semiconductor, but from technological point of view reveals materials ability to function at elevated temperatures. Several models have been proposed to describe the shift in the bandgap as a function of temperature; some from a strictly analytical point of view and a few have attempted to correlate the change in fundamental bandgap to physical parameters within the material. Among the most well – known models are those developed by Varshni (1967) [2], Viña (1984) [3], and Pässler (1997) [4].

A. Theoretical Models

The most frequently used model for fitting the fundamental bandgap as function of temperature was first proposed by Varshni [2] was an empirical relation to numerically fit measured data and is given by:

$$E_g(T) = E_g(0) - \frac{\alpha_v \cdot T^2}{\beta_v + T} \quad \text{Equation 2}$$

Where $E_g(0)$ is the bandgap at 0 K and α_v and β_v are fit parameters determined via modeling experimental data. This model represents a combination of linear high temperature dependence with a quadratic low temperature asymptote. There are several problems with this relation especially in the low temperature range; for example, this relation gives negative parameters for wide bandgap semiconductors [5] and does not have a physical correspondence to any defined material parameter. Although the beta is interpreted as dependent on the Debye temperature of

the semiconductor, no clear description has been defined in the available literature. For example, for a simple material such as GaAs it cannot even accurately describe measured data [6].

Another more recent model proposed by Viña et. al. [3] is a semi – empirical model to describe the temperature dependence of the bandgap, based upon the Bose – Einstein occupation distribution for phonons. It is describe by:

$$E_g(T) = E_g - \alpha_B \left(1 + \frac{2}{\exp\left(\frac{\theta_B}{T}\right) - 1} \right) \quad \text{Equation 3}$$

Where α_B represents the electron – phonon interaction, $\theta_B \equiv \hbar\omega/k_B$ is the characteristic temperature representing the effective phonon energy on the temperature scale, the bandgap at 0 K is represented as $E_g(0K) = E_g - \alpha_B$.

In 1997, Pässler [4] developed a analytical approach for determining the variation in the bandgap with temperature, represented by the following equation:

$$E_g(T) = E_g(0) - \frac{\alpha_p \theta_p}{2} \left[-1 + \sqrt{1 + \left(\frac{2T}{\theta_p}\right)^p} \right] \quad \text{Equation 4}$$

Where $E_g(0)$ is the bandgap at 0 K, $\alpha_p \equiv S(\infty) \equiv -\left.\frac{\partial E}{\partial T}\right|_{\lim T \rightarrow \infty}$ is the high – temperature limiting value for the forbidden gap entropy (this is similar to α_V in Equation 3), θ_p is a characteristic temperature parameter of the material representing the effective phonon energy ($\theta_p \equiv \hbar\omega/k_B$) in units of absolute temperature (similar to the value in the Viña model), and P is the empirical parameter related to the underlying spectral function of the electron – phonon interaction [6, 7].

According to aforementioned expressions, the Varshni and Viña models present three parameters to fit the experimentally measured bandgap data. Pässler demonstrated the inevitability of a fourth parameter in the expressions used to fit the temperature dependence of the bandgap shrinkage. Experimental data observed in the literature has shown non – linear dependence at low temperatures ($T < 30$ K) and linear dependencies at high temperature

($T > 100$ K). The main difference between these alternative models is the way in which they fit the low to intermediate range ($2 < T < 50$ K) [4]. In the low temperature range, the Varshni model leads to an overestimation of the measured temperature dependence, overestimating the bandgap at 0 K and the Viña model leads to an underestimation. This is because in this model a plateau behavior occurs. On the other hand by using the Pässler model an intermediate transition occurs and as shown in reference [6] allowing an improved fit to experimental data of several bulk and designed semiconductors. In the high temperature range all three models are almost indistinguishable and are usually considered interchangeable for high temperature modeling [8]. In this work, to compare the quality of fit for each of these models the standard approach it compares the squares of the theoretical curve from the experimental points. For this the standard Chi – squared equation is used [9]:

$$\Gamma^2 = \left(\frac{1}{n - m} \right) \sum_{i=1}^n (E_{g,i}^{\text{experimental}} - E_{g,i}^{\text{model}})^2 \quad \text{Equation 5}$$

Where the superscript indicates the experimental and modeled values the bandgap using the defined models for the i – th data point, $(n - m)$ is the number of degrees of freedom after fitting n data points with m variable in the model.

B. MWIR Results

The MWIR SL was grown via a solid source MBE on a residually P –type GaSb (001) substrate, it was designed to have nominally 7 MLs of InAs and 11 of GaSb. The PL was measured on a full P – I – N structure. The PL was measurements were made by using an Nd:YAG digitally pulsed laser and the pseudo – step scan technique. The samples were mounted into a sample – in – vapor cryostat equipped with a ZnSe cold window and KBr outer window. The laser excitation was measured to have peak intensity at 1082.6 nm and the spot size was focused to approximately 1 mm. To vary the laser intensity a series of neutral density filters were used to lower the laser power without changing its spectral or emission shape.

1. 10 Kelvin variation

At the lowest temperatures, PL is dominated by the lowest energy levels. For example, excitons (electrons and holes bound by the Coulomb interaction) and shallow impurity traps can often be discerned in the low temperature PL.

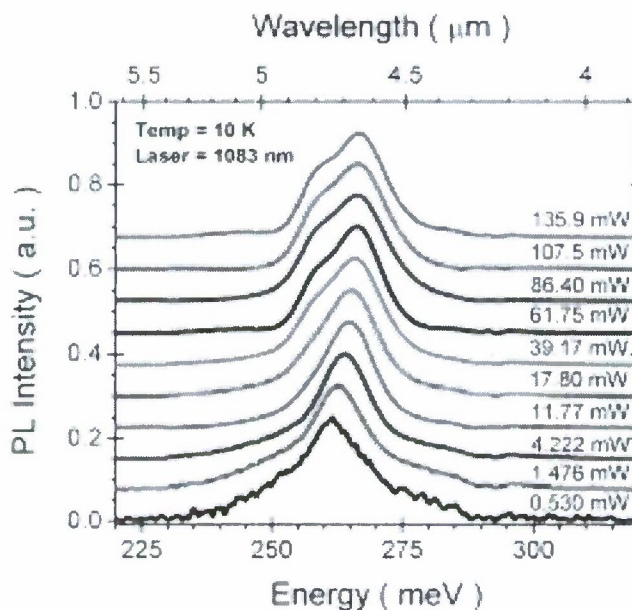


Figure 8: Excitation laser power dependence of the 10 K PL spectral of a MWIR SL sample; a partial list of the spectra are shown. The spectra are translated for better visualization

Figure 8 shows the PL dependence of the 10 K spectra as a function of laser excitation power. The spectrum shows that there are clearly two emission peaks, in Ref. [10] a similar split peak is also seen in the same material system. By increasing the laser power the second peak in the lower energy region appears to have a constant intensity with respect to the higher energy peak that matches with the ETBM model prediction for the actual value of the width of the bandgap.

The PL spectra shown in Figure 8 are fit by a pair of Gaussian peaks using the automated fitting algorithm from Micro Origin and are shown in Figure 9. At the highest laser power the automated fitting program is able to discern the two peaks with ease, but at the lowest laser power, in Figure 8, it cannot be fit automatically. In this case, the two peak's intensities are quite low and comparable. This is shown in the bottom right pane of Figure 9.

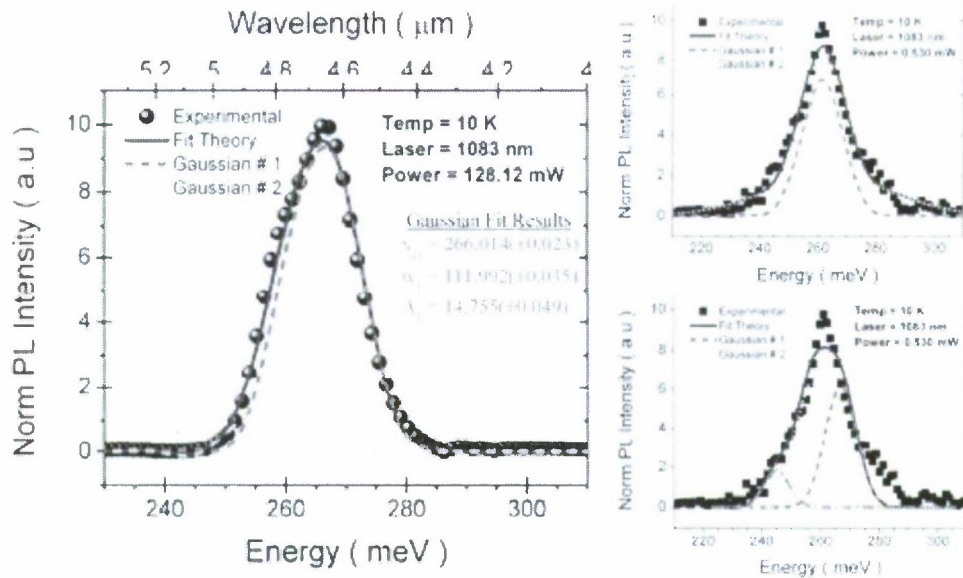


Figure 9: Gaussian fit of PL spectrum. The dashed lines are the individual peaks and circles are the measured data. The left pain is at high laser power and the right pains are at low excitation intensity.

To accomplish the fit, the peak position and width of the two main peaks from the higher power were used as the input and an additional lower energy peak is also added allowing only the intensity of the peaks to change. This new peak can be explained by an even lower energy defect state that has even a smaller population density that is saturated at low excitation intensity. Once the laser excitation is increased it can no longer be differentiated from the main two peaks, since it is completely filled and the extra population just broadens overshadowing its value.

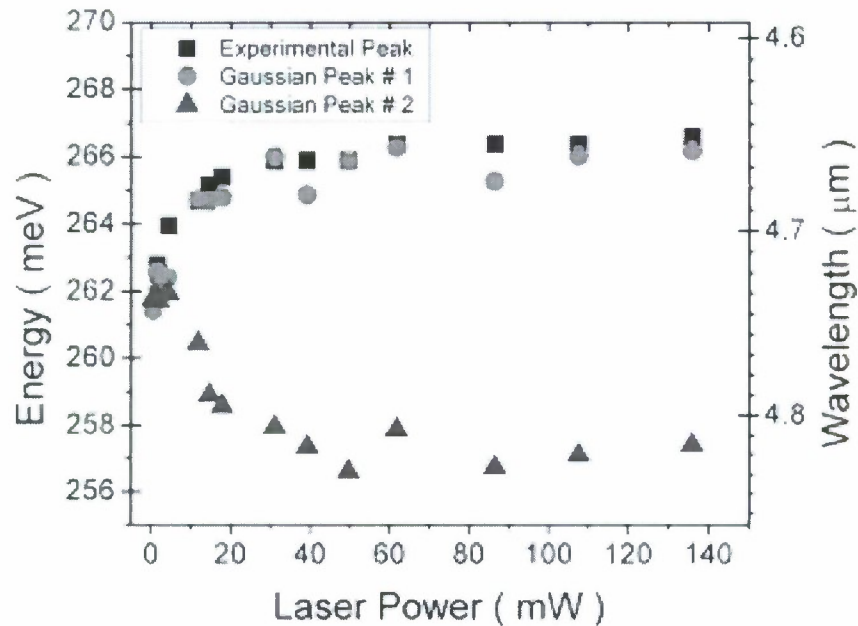


Figure 10: Result of two Gaussian fit of MWIR PL spectra measured at 10 K as function of emission intensity.

By plotting the measured maximum peak position in addition to the modeled peak centers from the Gaussian modeling, there is definitive separation of these two peaks of 8.34 meV, shown in Figure 10. Once the power is greater than 55 mW excitation power, the difference in the two peaks is revealed and below this value the automation in the fitting no longer works for the previously described reason. The fact that both peaks shift equally towards an average in the center expresses this fact clearly. The ~ 8 meV is similar to the donor impurity activation energy that was attained from C – V measurements of a sample from a similar growth design [11].

2. Intermediate Emission

As the sample's temperature and the corresponding thermal energy are increased, the carrier vacates the shallow traps reducing the intensity of the lower energy peak in the PL spectrum. At this point, it is important to note that the PL signal from any energy level depends on two parameters: the fractional population of the carriers and the density of the states participating in the radiative emission. Therefore, low energy traps that are few in number will appear in the low temperature regime because the thermal population of the higher density bands is small.

However, when the thermal population of band levels is appreciable, the dominant band – to – band transitions will dominate the PL because their states are more abundant.

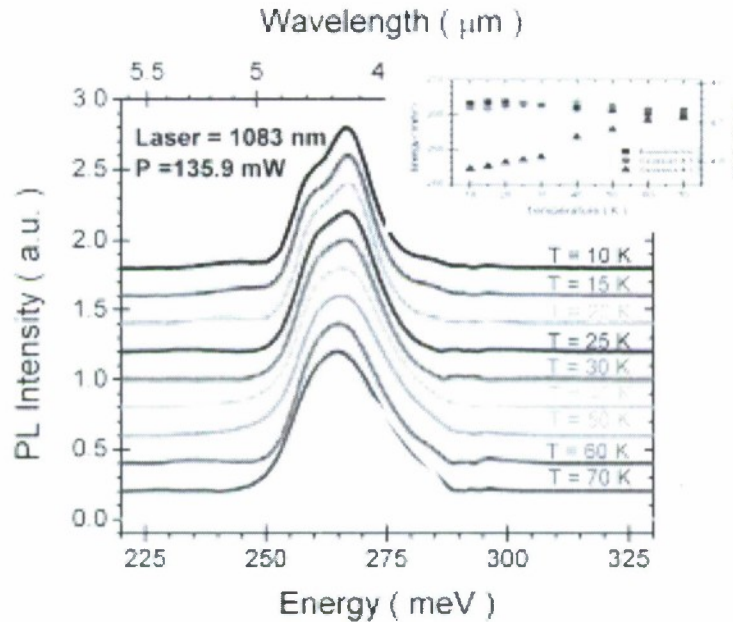


Figure 11: PL spectra as function of temperature for the range 10 to 77 K. The inset is the measured and modeled peak center.

When the PL is measured as a function of temperature, the main band – to – band emission persists while the lower energy defect peak broadens and is no longer well defined. This fact reinforces the idea that the lower energy peak is due to an impurity band, while the higher energy peak remains until 300 K (as shown in Figure 11).

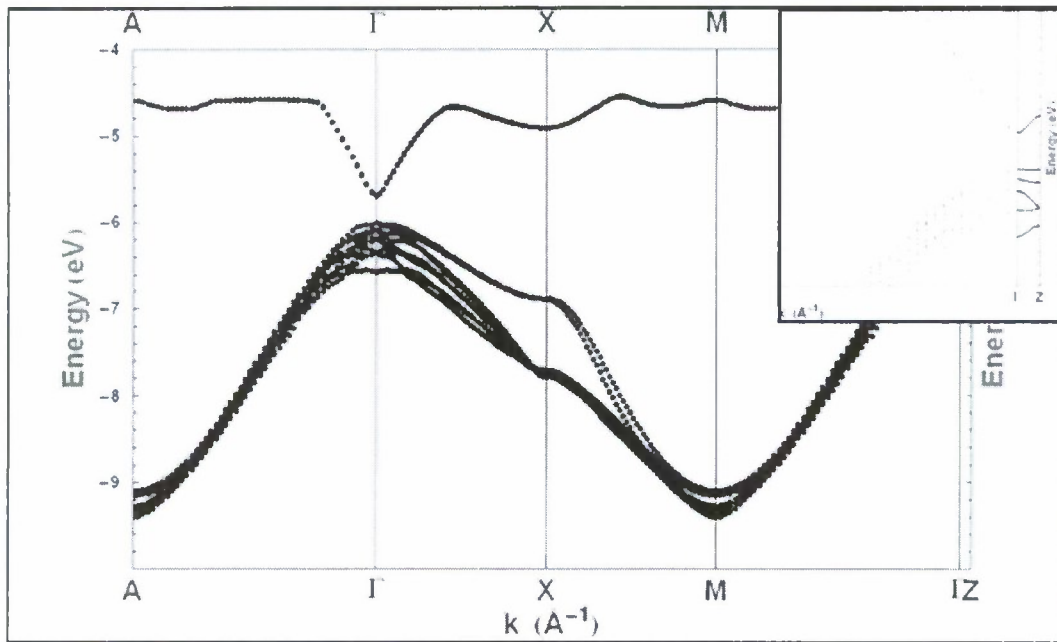


Figure 12: Band Structure of the 7 ML InAs/11 ML GaSb Superlattice based upon the sps* ETBM model [12]. The inset is a zoom - in of the Gamma - point.

Another possibility for the lower energy peak is that interface roughness is causing a defect that would make the band structure near the Gamma - point narrower and dragged into the forbidden bandgap (shown in Figure 12). Both possibility of interface roughness and impurity contribution are still under investigation. To study if this peak were due to the material one proposed study is perform the PL with the samples that were not grown into full p - i - n structures but to grow 1 μm thick SL stacks without doping and various doping levels and doping techniques to compare if this would effect the low energy peak, by creating or nullify a Fermi or band edge tailing state. To better calibrate this doping level a carrier concentration measure would be beneficial, but not required for a relative comparison.

3. Band - to - Band Emission between 10 to 300 K

The asymmetry in the spectrum in Figure 13 is due to the thermal distribution of the carrier in the conduction band and increases with the either the increase in excitation power (Figure 14) or with increasing temperature.

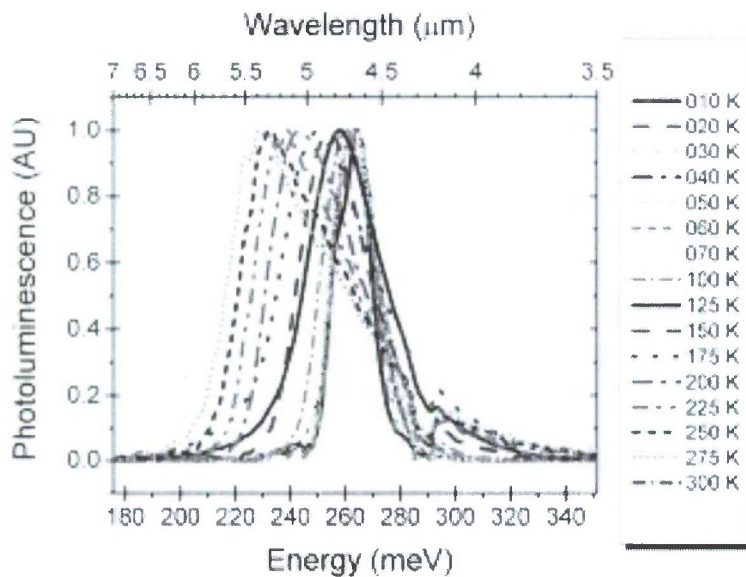


Figure 13: PL spectra for temperature range from 10 to 300 K with an excitation of 135.9 mW.

As the temperature increases, the population of the conduction and valence bands redistributes due to thermal fluctuation and is commonly observed in PL measurements with temperature variation. By increasing temperature the band gap energy reduces. This is most significant in the higher temperature region and must be accounted for when designing a device for high temperature operation.

4. Fit of MWIR Experimental Results

Figure 14 shows the peak taken from the Gaussian Fit of the PL spectra; the lines are from the modeling of three described models described in Equation 2, Equation 3, and Equation 4. In the large scale all three models appear to show the same variation in bandgap, but by studying the inset the evidence in the weakness of the earlier models is apparent.

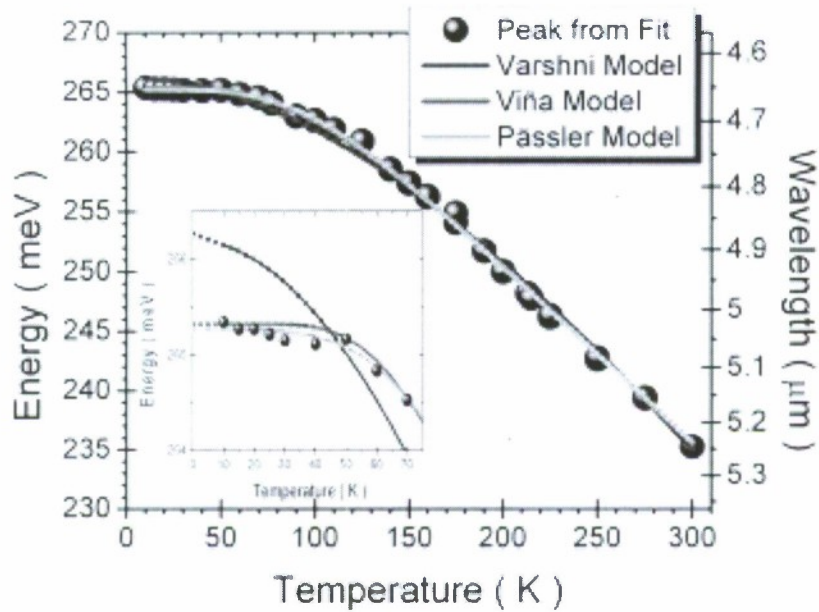


Figure 14: Plot of bandgap renormalization of main Gaussian peak plus fit of modeling using the Varshni, Viña, and Pässler models. The inset is a zoom – in of the low temperature region.

The Viña underestimates the low temperature bandgap and the Varshni overestimates the variation. The Pässler model represents the best adjustment to the bandgap shift. This is not only due to the additional parameter, but also it is better to take into account real material parameters such as the phonon contribution.

Table I: Obtained parameter for modeling the PL peak dependence with temperature.

Model	$E_g(0)$ [meV]	α_v [meV/K]	β [K]	p	Γ^2
	E_B [meV]	α_B [meV]	θ [K]		
Varshni	266.20(± 0.257)	0.328(± 0.069)	647.42(± 104)	---	0.518
Viña	289.82(± 1.56)	24.498($\pm 0.1.65$)	291.285(± 12.034)	---	0.239
Pässler	265.28(± 0.17)	0.15(± 0.0052)	208.45(± 11.98)	4.05(± 0.604)	0.198

Table I shows the parameters obtained from modeling the bandgap as function of temperature for the MWIR sample. In the table are all parameter plus the Chi –squared value obtained for the fits to compare the quality of the fits. It is clear that the Pässler model best replicates the experimental data.

VI. Thermal Population Variation

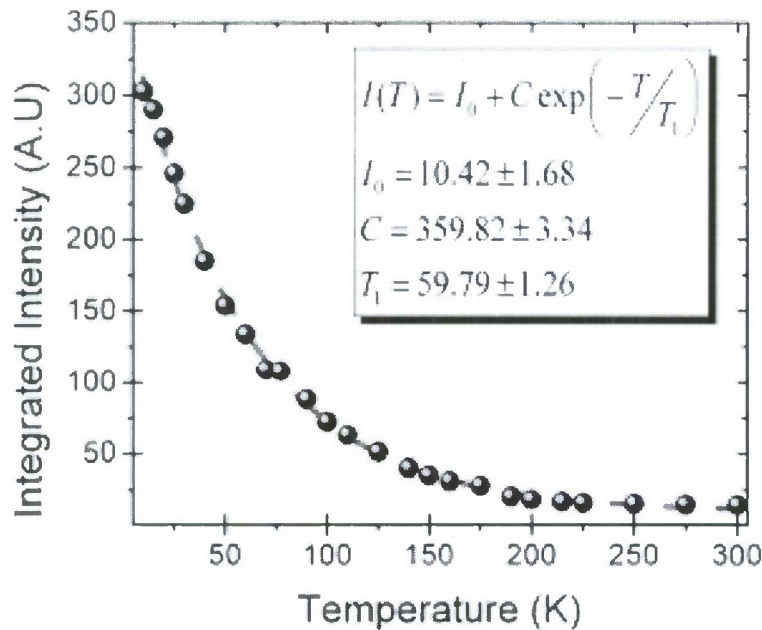


Figure 15: Temperature – dependent integrated photoluminescence intensity for the MWIR superlattice.

In addition to the population increase in discrete states, thermal distributions are manifested in the PL line width of the band edge transitions. In this sample the FWHM of the PL spectrum increases in a linear fashion from 7.365 meV to 38.06 meV from 10 to 300 K. When $k_B T$ exceeds the inhomogeneous broadening of the sample, a high energy Boltzmann tail appears in the PL spectrum. This feature can be useful for estimating the local temperature of the sample. Unfortunately, thermal quenching can hide sparse low energy states and thermal broadening can obscure important details in the spectrum such as the position of the forbidden bandgap. Due to this emission broadening, the photoluminescence experiments to determine material quality are performed at low temperature.

In the characterization of discrete low – energy states, quantitative analysis of the decrease in the PL intensity with temperature can be used to measure the depth of the trap. By plotting the PL intensity vs. temperature, the slope yields the activation temperature of the excited carriers. This form of graph is an Arrhenius plot as shown in Figure 15. Although the T_1 is less than that published in Ref. [13], it is comparable values that of other groups. The higher value can be explained in one of two ways: (1) the laser wavelength is half that of the Nd:YAG

laser used here and (2) in Ref. [13] a grating monochrometer was used so the values recorded were a narrow wavelength of the peak at 3.7 μm while by using an FTS the signal recorded was the signal across the entire measurement band.

VII. Summary

Photoluminescence analysis is a powerful tool in the characterization of semiconductors. Although there are a number of experimental techniques to provide information on materials, in the optoelectronics industry detailed analysis of the optical and electrical properties is vital. Mechanical information is useful because it is closely correlated with these properties, but PL measurements explore the electronic features directly. Other techniques can provide similar access, but they typically require more sophisticated excitation or detection schemes.

The PL spectrum gives precise information on the energy levels available to the electrons in the material because PL emission is the result of the optical transitions between the narrow electronic states and unlike absorption will only give information on the minimum transition level. The intensity of the PL signal depends on the rate of the radiative and non – radiative events that in turn depends on the density of the non – radiative states.

PL measurements are not sensitive to the experimental setup, which makes PL an excellent probe to material modification. Variation in the PL signal with external parameters such as temperature can help to determine material quality. Temperature – dependent thermal activation of the electronic states can be used to observe their position in comparison to the conduction and valence bands.

Applications of PL analysis range from simple spatial scans of wafer growths to exhaustive investigation of excitation – intensity dependent PL in a material. Furthermore, new PL techniques continue to emerge such as polarization dependence continues to expand the flexibility of PL analysis. PL is well suited to studying bulk materials as well as engineered materials to determine the affect of interfaces and surfaces. Interfaces are of great importance in new optoelectronic materials where layered structures are becoming more complex. Although PL measurements have their complexities in gaining direct insight into these material, it is still a vital measurement technique for improving layered structure such as the one studied in this

work, InAs/GaSb superlattices. It is still the fastest way to determine initial results for quick feedback to make growth modifications, such as interface modification or ratios of flux densities.

VIII. References:

1. Smith, K.K., *Photoluminescence of semiconductor materials*. Thin Solid Films, 1981. **84**(2): p. 171-182.
2. Varshni, Y.P., *Temperature dependence of the energy gap in semiconductors*. Physica, 1967. **34**(1): p. 149-154.
3. Vina, L., S. Logothetidis, and M. Cardona, *Temperature dependence of the dielectric function of germanium*. Physical Review B, 1984. **30**(4): p. 1979.
4. Passler, R. and G. Oelgart, *Appropriate analytical description of the temperature dependence of exciton peak positions in GaAs/Al_xGa_{1-x}As multiple quantum wells and the Gamma_{8v} - Gamma_{6c} gap of GaAs*. Journal of Applied Physics, 1997. **82**(5): p. 2611-2616.
5. Grilli, E., et al., *High-precision determination of the temperature dependence of the fundamental energy gap in gallium arsenide*. Physical Review B, 1992. **45**(4): p. 1638.
6. Passler, R., *Temperature dependence of fundamental band gaps in group IV, III-V, and II-VI materials via a two-oscillator model*. Journal of Applied Physics, 2001. **89**(11): p. 6235-6240.
7. Passler, R., *Basic moments of phonon density of states spectra and characteristic phonon temperatures of group IV, III-V, and II-VI materials*. Journal of Applied Physics, 2007. **101**(9): p. 093513-12.
8. Caballero-Rosas, A., et al., *Temperature dependence of optical transitions in Al_xGa_{1-x}As/GaAs quantum well structures grown by molecular beam epitaxy*. Thin Solid Films, 2005. **490**(2): p. 161-164.
9. Bevington, P.R., *Data Reduction and Error Analysis of the Physical Science*. 1968, New York: McGraw-Hill.
10. Haugan, H.J., et al., *Pushing the envelope to the maximum: Short-period InAs/GaSb type-II superlattices for mid-infrared detectors*. Physica E: Low-dimensional Systems and Nanostructures, 2006. **32**(1-2): p. 289-292.
11. Hood, A., et al., *Capacitance-voltage investigation of high-purity InAs/GaSb superlattice photodiodes*. Applied Physics Letters, 2006. **88**(5): p. 052112-3.
12. Wei, Y. and R. Manijeh, *Modeling of type-II InAs/GaSb superlattices using an empirical tight-binding method and interface engineering*. Physical Review B (Condensed Matter and Materials Physics), 2004. **69**(8): p. 085316.
13. Wei, Y., et al., *High quality type II InAs/GaSb superlattices with cutoff wavelength $\sim 3.7 \mu m$ using interface engineering*. Journal of Applied Physics, 2003. **94**(7): p. 4720-4722.